

Computation of integral invariants for geometry processing with applications to analysis of broken bone fragments

Jeff Calder

School of Mathematics
University of Minnesota

Symposium on Computational Modeling and Image Processing of
Biometrical Problems
June 15–17, 2019

This research was supported by NSF-DMS grant 1816917.

Outline

1 Background

- Broken bones
- Differential and integral invariants

2 Spherical Volume Invariant

- Boundary integral formulation
- Computation
- PCA on local neighborhoods
- Experimental results

3 References

Outline

1 Background

- Broken bones
- Differential and integral invariants

2 Spherical Volume Invariant

- Boundary integral formulation
- Computation
- PCA on local neighborhoods
- Experimental results

3 References

Outline

1 Background

- Broken bones
- Differential and integral invariants

2 Spherical Volume Invariant

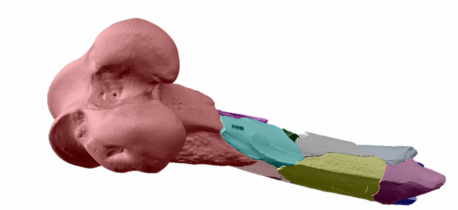
- Boundary integral formulation
- Computation
- PCA on local neighborhoods
- Experimental results

3 References

Why/how do bones break?

Main research queries:

- 1 How do broken bone fragments fit back together?



- 2 What broke them?
 - ▶ E.g., Animal, hominin, or natural causes?

Collaboration with Professor Peter Olver (Mathematics, UMN), Professor Martha Tappen (Anthropology, UMN), Katrina Yezzi-Woodley, Riley O'Neill, Pedro Angulo-Umana, Bo Hessburg, Jacob Elafandi, Jacob Theis, and Cheri Shakiban.

When did humans first come to North America?

Anthropology

This article is more than 2 years old

Could history of humans in North America be rewritten by broken bones?

Smashed mastodon bones show humans arrived over 100,000 years earlier than previously thought say researchers, although other experts are sceptical

Ian Sample Science editor

@iansample

Wed 26 Apr 2017 13:00 EDT



Researchers present some of the arguments for and against the new evidence.



Editorially independent, open to everyone

We chose a different approach – will you support it?

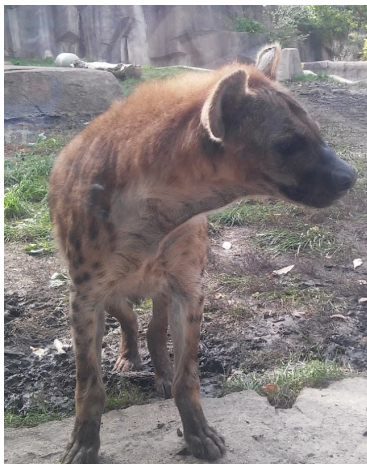
Support The Guardian →

Key finding: Bones appear to have been broken by humans with stone tools, though this is **highly controversial** in anthropology.

Questions

- 1 Does the bone fragment shape tell us anything about the actor responsible for the fragmentation?
- 2 If so, can we distinguish hominin damage from carnivore damage?
- 3 Further, can we identify different types of hominin damage?

Breaking bones: Animal

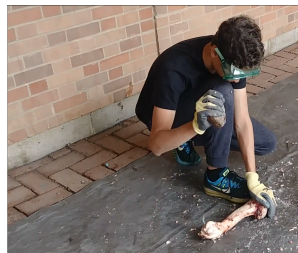


Crocuta crocuta = hyena

Breaking bones: Rockfall



Breaking bones: Hominin



Batting, Hammerstone & Anvil, Hammerstone

Outline

1 Background

- Broken bones
- Differential and integral invariants

2 Spherical Volume Invariant

- Boundary integral formulation
- Computation
- PCA on local neighborhoods
- Experimental results

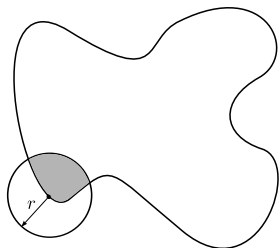
3 References

Differential invariants of curves/surfaces

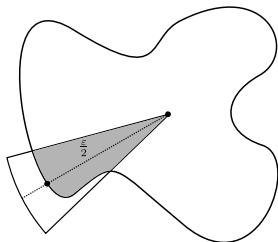
- Long history of differential invariants in shape processing
 - ▶ Mean and Gauss curvature of surfaces, etc.
- Applications:
 - ▶ Shape recognition and matching
 - ▶ Feature extraction
- **Advantages:** Well-understood from differential geometry, and established uniqueness of representations.
- **Disadvantages:** Lack of robustness to noise.

Integral Invariants

- Integral invariants involve integrals of the curve/surface [Manay et al., 2004]



(a) Circular area invariant



(b) Cone area invariant

- **Advantage:** Automatically robust to noise.
- **Disadvantage:** Not much theory. Uniqueness of representations?
 - ▶ [Calder and Esedoğlu, 2012]

Outline

- 1 Background
 - Broken bones
 - Differential and integral invariants

- 2 Spherical Volume Invariant
 - Boundary integral formulation
 - Computation
 - PCA on local neighborhoods
 - Experimental results

- 3 References

Spherical volume invariant

Definition (Spherical volume invariant)

Consider a closed surface $S \subset \mathbb{R}^3$ bounding a domain $\Omega = \text{int } S$. We define the **spherical volume invariant** at each point $p \in S$ to be

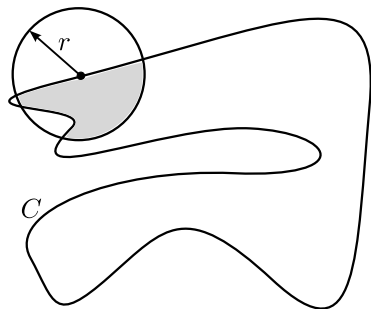
$$V_{S,r}(p) = \text{Vol}(\Omega \cap B_r(p)),$$

- Used for feature extraction
[Yang et al., 2006, Pottmann et al., 2009, Pottmann et al., 2007]
- Relation to **Mean Curvature**:

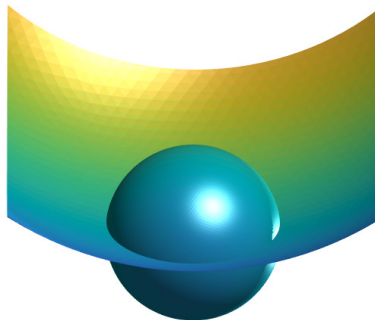
$$V_{S,r}(p) = \frac{2}{3}\pi r^3 - \frac{1}{4}\pi H(p)r^4 + \mathcal{O}(r^5) \quad \text{as } r \rightarrow 0,$$

where $H(p)$ is the mean curvature of S at p .

Circular area and spherical volume invariants



(c) Circular Area Invariant



(d) Spherical Volume Invariant

Outline

- 1 Background
 - Broken bones
 - Differential and integral invariants

- 2 Spherical Volume Invariant
 - **Boundary integral formulation**
 - Computation
 - PCA on local neighborhoods
 - Experimental results

- 3 References

How to compute?

Two existing methods:

- 1 FFT methods, based on rewriting as a convolution

$$V_{S,r}(p) = \chi_{\Omega} * \chi_{B_r}.$$

- 2 Direct numerical integration, e.g., the octree method

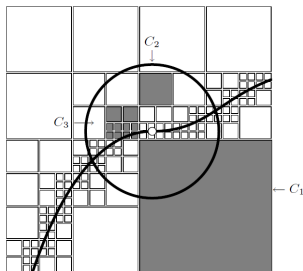


Figure 8: Integral invariant computation based on an octree data structure. The cubes C_1 , C_2 , C_3 correspond to cases $2c\alpha$, $2b$, and $2c\beta$ of Algorithm 1, respectively.

[Yang et al., 2006, Pottmann et al., 2009, Pottmann et al., 2007]

Question: Can we restrict the computation to the surface S , and avoid discretizing the ambient space?

Main idea: Divergence theorem

Fix $p = 0$ and write $B_r = B_r(0)$ and $V_{S,r} = V_{S,r}(0)$.

Let \mathbf{V} be a vector field with $\operatorname{div} \mathbf{V} = 1$ so that

$$V_{S,r} = \int_{\Omega \cap B_r} \operatorname{div} \mathbf{V} \, dx = \int_{S \cap B_r} \mathbf{V} \cdot \nu \, dS + \int_{\Omega \cap \partial B_r} \mathbf{V} \cdot \nu \, dS.$$

Main idea: Divergence theorem

Fix $p = 0$ and write $B_r = B_r(0)$ and $V_{S,r} = V_{S,r}(0)$.

Let \mathbf{V} be a vector field with $\operatorname{div} \mathbf{V} = 1$ so that

$$V_{S,r} = \int_{\Omega \cap B_r} \operatorname{div} \mathbf{V} \, dx = \int_{S \cap B_r} \mathbf{V} \cdot \nu \, dS + \int_{\Omega \cap \partial B_r} \mathbf{V} \cdot \nu \, dS.$$

Can we find a smooth vector field \mathbf{V} satisfying

$$\begin{cases} \operatorname{div} \mathbf{V} = 1 & \text{in } B_r \\ \mathbf{V} \cdot \nu = 0 & \text{on } \partial B_r \end{cases} ?$$

Short answer: No, since

$$\int_{B_r} \operatorname{div} \mathbf{V} \, dx = \int_{\partial B_r} \mathbf{V} \cdot \nu \, dS.$$

Conversion to Poisson problem

Let's make an ansatz (in \mathbb{R}^n)

$$\mathbf{V}(x) = \frac{1}{n}x + \nabla u$$

where $u : B_r \rightarrow \mathbb{R}$. Then $\operatorname{div} \mathbf{V} = 1 + \Delta u$ and the problem

$$\begin{cases} \operatorname{div} \mathbf{V} = 1 & \text{in } B_r \\ \mathbf{V} \cdot \nu = 0 & \text{on } \partial B_r \end{cases}$$

is reduced to

$$\boxed{\begin{cases} \Delta u = 0 & \text{in } B_r \\ \frac{\partial u}{\partial \nu} = -\frac{r}{n} & \text{on } \partial B_r, \end{cases}}$$

since $\nu = x/r$.

Solving the Poisson problem

To make the Poisson problem solvable, we add a source

$$\begin{cases} -\Delta u = \alpha_n r^n \delta & \text{in } B_r \\ \frac{\partial u}{\partial \nu} = -\frac{r}{n} & \text{on } \partial B_r, \end{cases}$$

where $\alpha_n = |B_1|$. The solution is

$$u(x) = \alpha_n r^n \Phi(x),$$

where Φ is the fundamental solution of Laplace's equation

$$\Phi(x) = \begin{cases} -\frac{1}{2\pi} \log |x|, & \text{if } n = 2 \\ \frac{1}{n(n-2)\alpha_n |x|^{n-2}}, & \text{if } n \geq 3 \end{cases}$$

This gives

$$\mathbf{V}(x) = \frac{1}{n} x - \frac{r^n}{n} \frac{x}{|x|^n}.$$

Back to the divergence theorem

Set $\mathbf{V}(x) = \frac{1}{n}x - \frac{r^n}{n} \frac{x}{|x|^n}$ and compute for $0 < \varepsilon < r$

$$\begin{aligned} \int_{S \cap (B_r \setminus B_\varepsilon)} \mathbf{V} \cdot \nu \, dS &= \int_{\partial(\Omega \cap (B_r \setminus B_\varepsilon))} \mathbf{V} \cdot \nu \, dS + \int_{\Omega \cap \partial B_\varepsilon} \mathbf{V} \cdot \nu \, dS \\ &= \int_{\Omega \cap (B_r \setminus B_\varepsilon)} \operatorname{div} \mathbf{V} \, dx + \int_{\Omega \cap \partial B_\varepsilon} \left(\frac{\varepsilon}{n} - \frac{r^n}{n \varepsilon^{n-1}} \right) dS \\ &= \int_{\Omega \cap (B_r \setminus B_\varepsilon)} dx + \left(\frac{\varepsilon}{n} - \frac{r^n}{n \varepsilon^{n-1}} \right) \mathcal{H}^{n-1}(\Omega \cap \partial B_\varepsilon) \\ &= V_{S,r} - V_{S,\varepsilon} + \left(\frac{\varepsilon}{n} - \frac{r^n}{n \varepsilon^{n-1}} \right) \mathcal{H}^{n-1}(\Omega \cap \partial B_\varepsilon), \end{aligned}$$

where \mathcal{H}^{n-1} denotes $(n-1)$ -dimensional Hausdorff measure. Therefore

$$V_{S,r} = V_{S,\varepsilon} + \frac{1}{n} \int_{S \cap (B_r \setminus B_\varepsilon)} \left(1 - \frac{r^n}{|x|^n} \right) (x \cdot \nu) \, dS + \alpha_n (r^n - \varepsilon^n) \frac{\mathcal{H}^{n-1}(\Omega \cap \partial B_\varepsilon)}{\mathcal{H}^{n-1}(\partial B_\varepsilon)}.$$

Main Result

Theorem ([O'Neill et al., 2019])

Let $\Omega \subset \mathbb{R}^n$ be open and bounded with Lipschitz boundary $S := \partial\Omega$. Let $p \in S$ and assume the limit

$$(1) \quad \Gamma(p) := \lim_{\varepsilon \rightarrow 0^+} \frac{\mathcal{H}^{n-1}(\Omega \cap \partial B_\varepsilon(p))}{\mathcal{H}^{n-1}(\partial B_\varepsilon(p))}$$

exists. Then we have

$$(2) \quad V_{S,r}(p) = \frac{1}{n} \int_{S \cap B_r(p)} \left(1 - \frac{r^n}{|x-p|^n}\right) (x-p) \cdot \nu \, dS + \alpha_n r^n \Gamma(p).$$

- If S is differentiable at p then $\Gamma(p) = \frac{1}{2}$.
- If S is a triangulated mesh, $\Gamma(p)$ exists and

$$(x-p) \cdot \nu = 0$$

for x in the vertex polygon of p , so the kernel in (2) is integrable.

Outline

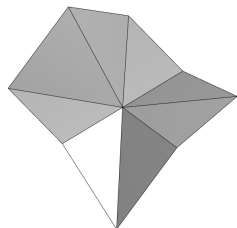
- 1 Background
 - Broken bones
 - Differential and integral invariants

- 2 Spherical Volume Invariant
 - Boundary integral formulation
 - **Computation**
 - PCA on local neighborhoods
 - Experimental results

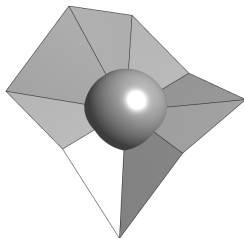
- 3 References

Computing $\Gamma(p)$

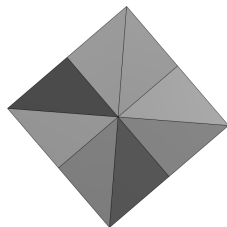
$$\Gamma(p) := \lim_{\varepsilon \rightarrow 0^+} \frac{\mathcal{H}^{n-1}(\Omega \cap \partial B_\varepsilon(p))}{\mathcal{H}^{n-1}(\partial B_\varepsilon(p))}.$$



(e) Vertex triangles



(f) Small sphere



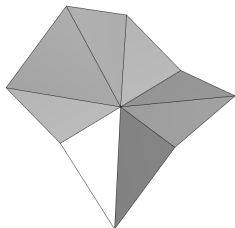
(g) From above

Computing $\Gamma(p)$

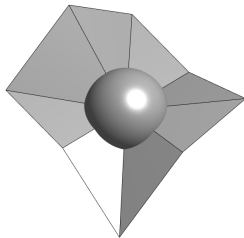
$$\Gamma(p) = \frac{1}{2} - \frac{1}{4\pi} \sum_{i=1}^k \arcsin(d_i \sin(\theta_{i+1} - \delta_i)) - \arcsin(d_i \sin(\theta_i - \delta_i)),$$

where

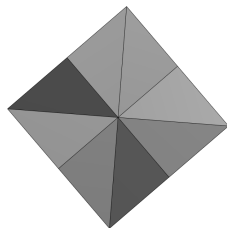
$$d_i = \sqrt{(\nu_1^i)^2 + (\nu_2^i)^2}, \quad \delta_i = \text{atan2}(\nu_2^i, \nu_1^i), \quad \text{and } \theta_i = \text{atan2}(y_i, x_i).$$



(h) Vertex triangles



(i) Small sphere



(j) From above

Numerical integration

Recall

$$V_{S,r}(p) = \frac{1}{n} \int_{S \cap B_r(p)} \left(1 - \frac{r^3}{|x-p|^3} \right) (x-p) \cdot \nu \, dS + \alpha_3 r^3 \Gamma(p).$$

Assume S is a triangulated mesh. Then we need to compute

$$I := \int_T \left(1 - \frac{r^3}{|x|^3} \right) x \cdot \nu \, dS,$$

where $T \subset \mathbb{R}^3$ is a planar triangle with $0 \notin T$. Note that

$$I = (z \cdot \nu) |T| - r^3 (z \cdot \nu) \int_T \frac{1}{|x|^3} \, dx,$$

for any $z \in T$. This is a **hypersingular integral**.

Explicit expressions for 3D boundary integrals in potential theory[†]

S. Nintcheu Fata*[†]

*Computer Science and Mathematics Division, Oak Ridge National Laboratory, P.O. Box 2008,
MS 6367, Oak Ridge, TN 37831-6367, U.S.A.*

SUMMARY

On employing isoparametric, piecewise linear shape functions over a flat triangular domain, exact expressions are derived for all surface potentials involved in the numerical solution of three-dimensional singular and hyper-singular boundary integral equations of potential theory. These formulae, which are valid for an arbitrary source point in space, are represented as analytic expressions over the edges of the integration triangle. They can be used to solve integral equations defined on polygonal boundaries via the collocation method or may be utilized as analytic expressions for the inner integrals in the Galerkin technique. In addition, the constant element approximation can be directly obtained with no extra effort. Sample problems solved by the collocation boundary element method for the Laplace equation are included to validate the proposed formulae. Copyright © 2008 John Wiley & Sons, Ltd.

Received 15 May 2008; Revised 11 July 2008; Accepted 21 August 2008

KEY WORDS: analytic integration; singular integrals; boundary integral method; triangular boundary; potential theory

Let $x^* \in \mathbb{R}^3$ denote the orthogonal projection of the origin onto the plane P containing T . Let $x^1, x^2, x^3 \in \mathbb{R}^3$ be the vertices of T and write $x^4 = x^1$. Define

$$(3) \quad \theta = \begin{cases} 0, & \text{if } x^* \in P \setminus \overline{T} \\ \pi, & \text{if } x^* \in \partial T \setminus \{x^1, x^2, x^3\} \\ 2\pi, & \text{if } x^* \in T \\ \theta_i, & \text{if } x^* = x^i, \end{cases}$$

where θ_i is the interior angle of T at the vertex x^i .

Let L^i denote the oriented edge of the triangle T from x^i to x^{i+1} . Associated with each edge L^i , we construct an orthonormal basis (e_1^i, e_2^i) for the plane P with origin x^* , e_1^i taken in the direction of the edge L^i , and $e_2^i = \nu \times e_1^i$ chosen so that (e_1^i, e_2^i, ν) is an orthonormal basis for \mathbb{R}^3 . Let

$$p_i^j = (x^j - x^*) \cdot e_1^i, \quad q_i^j = (x^j - x^*) \cdot e_2^i,$$

be the planar coordinates of the vertex x^j in the basis (e_1^i, e_2^i) . By definition, $q_1^1 = q_2^1$, $q_2^2 = q_3^2$, and $q_3^3 = q_4^3$, since the vertices x^j and x^{j+1} lie along the line spanned by e_1^j . We denote the common values as

$$q_i := q_i^i = q_i^{i+1}.$$

Finally, set $\eta = x^1 \cdot \nu$, noting that $\eta \neq 0$, since $0 \notin T$. We then define

$$(4) \quad \gamma_i = \arctan \left(\frac{-2p_i^i q_i \eta |x^i|}{(q_i)^2 |x^i|^2 - (p_i^i)^2 \eta^2} \right) - \arctan \left(\frac{-2p_i^{i+1} q_i \eta |x^{i+1}|}{(q_i)^2 |x^{i+1}|^2 - (p_i^{i+1})^2 \eta^2} \right).$$

The hypersingular integral is now given by

$$(5) \quad \int_T \frac{1}{|x|^3} dx = \frac{\gamma_1 + \gamma_2 + \gamma_3 + 2 \operatorname{sign}(\eta) \theta}{2\eta}.$$

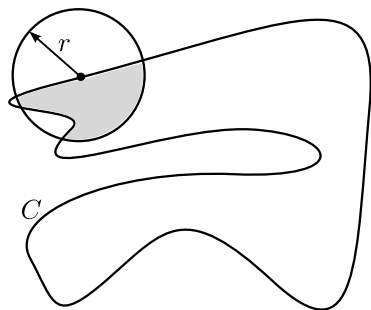
Outline

- 1 Background
 - Broken bones
 - Differential and integral invariants

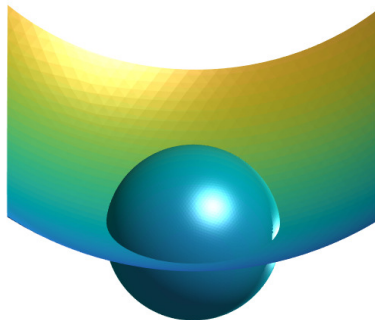
- 2 Spherical Volume Invariant
 - Boundary integral formulation
 - Computation
 - PCA on local neighborhoods
 - Experimental results

- 3 References

Circular area and spherical volume invariants



(k) Circular Area Invariant



(l) Spherical Volume Invariant

PCA on local neighborhoods

In order to capture more information about the surface, we follow [Pottmann et al., 2007] and perform PCA on the set region $\Omega \cap B_r(p)$:

$$M_{S,r}(p) := \int_{\Omega \cap B_r(p)} (x - \bar{x}(p))(x - \bar{x}(p))^T dx,$$

where

$$\bar{x}(p) := \frac{1}{V_{S,r}(p)} \int_{\Omega \cap B_r(p)} x dx.$$

The eigenvalues of $M_{S,r}(p)$ have the asymptotic expansions

$$\begin{aligned}\lambda_1(p) &= \frac{2\pi}{15} r^5 - \frac{\pi}{48} [3\kappa_1(p) + \kappa_2(p)] r^6 + \mathcal{O}(r^7) \\ \lambda_2(p) &= \frac{2\pi}{15} r^5 - \frac{\pi}{48} [\kappa_1(p) + 3\kappa_2(p)] r^6 + \mathcal{O}(r^7) \\ \lambda_3(p) &= \frac{19\pi}{480} r^5 - \frac{9\pi}{512} [\kappa_1(p) + \kappa_2(p)] r^6 + \mathcal{O}(r^7),\end{aligned}$$

as $r \rightarrow 0$, where $\kappa_1(p), \kappa_2(p)$ are the principal curvatures of the surface S at the point $p \in S$.

PCA on local neighborhoods

To compute $M_{S,r}(p)$ we just need to compute

$$(6) \quad m_i(p) := \int_{\Omega \cap B_r(p)} (x_i - p_i) dx, \text{ and } c_{ij}(p) := \int_{\Omega \cap B_r(p)} (x_i - p_i)(x_j - p_j) dx.$$

Lemma ([O'Neill et al., 2019])

Let us abbreviate $y = x - p$. Then, for any $1 \leq i, j \leq n$, we have

$$(7) \quad m_i(p) = \frac{1}{n+1} \int_{S \cap B_r(p)} (y_i y - r^2 e_i) \cdot \nu dS(x).$$

and

$$(8) \quad c_{ij}(p) = \frac{r^2}{n+2} V_{S,r}(p) \delta_{ij} + \frac{1}{2n+4} \int_{S \cap B_r(p)} (2y_i y_j y - r^2 (y_j e_i + y_i e_j)) \cdot \nu dS(x).$$

Outline

- 1 Background
 - Broken bones
 - Differential and integral invariants

- 2 Spherical Volume Invariant
 - Boundary integral formulation
 - Computation
 - PCA on local neighborhoods
 - Experimental results

- 3 References

Experimental results

CPU time on Stanford dragon

Mesh size (# triangles/#vertices)	Radius					
	$r = 0.5$	$r = 1$	$r = 2$	$r = 3$	$r = 4$	$r = 5$
45,360/22,678	0.19s	0.69s	2.5s	6.1s	10.3s	16.8s
90,722/45,359	0.67s	2.1s	8.9s	26.2s	40.7s	66.7s
181,444/90,720	2.0s	7.8s	32.8s	83.3s	151.4s	268.4s

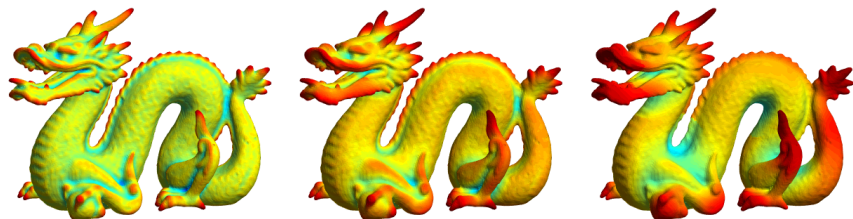


Figure: Spherical volume invariant for radii of 1, 2, and 5.

Experimental results

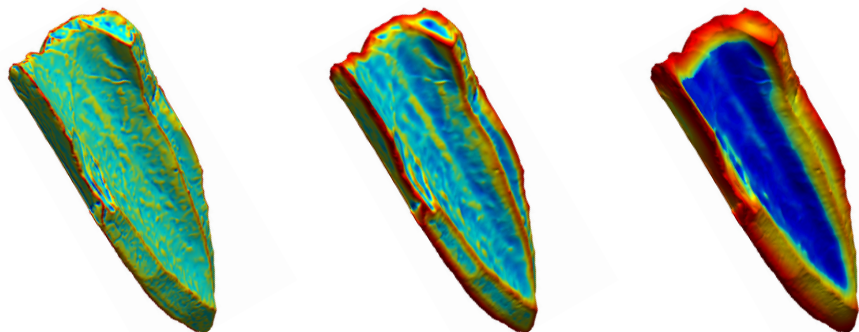


Figure: Spherical volume invariant computed at radii of 1, 2, and 5.

Experimental results

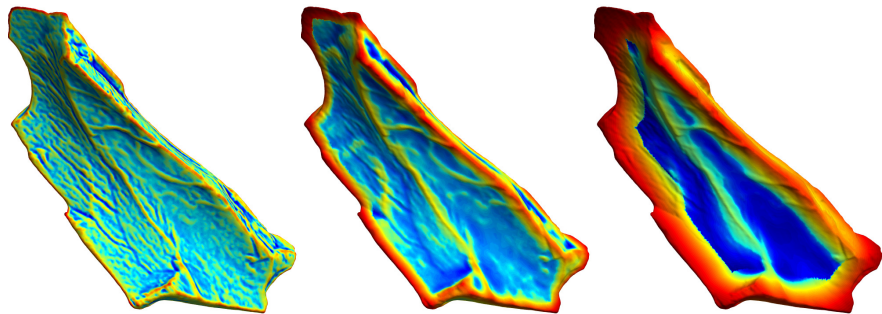


Figure: Spherical volume invariant computed at radii of 1, 2, and 5.

Experimental results

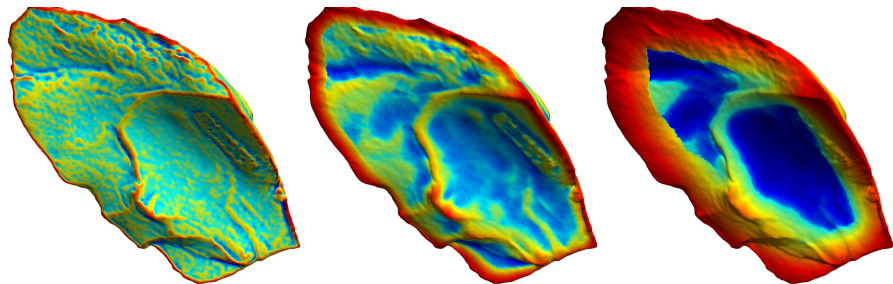


Figure: Spherical volume invariant computed at radii of 1, 2, and 5.

Experimental results

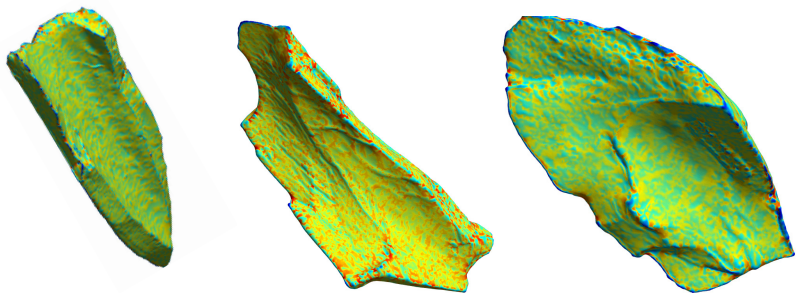


Figure: Gauss curvature with $r = 0.5$.

Experimental results

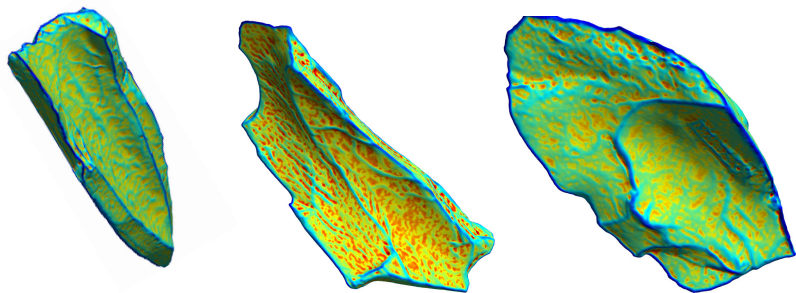


Figure: Principal curvature κ_1 with $r = 0.5$.

Experimental results

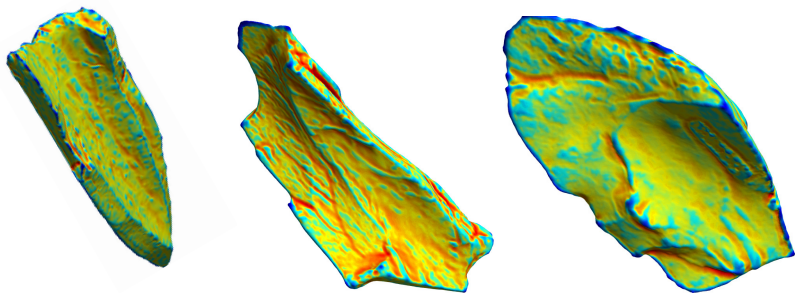


Figure: Principal curvature κ_2 with $r = 0.5$.

Fracture edge detection

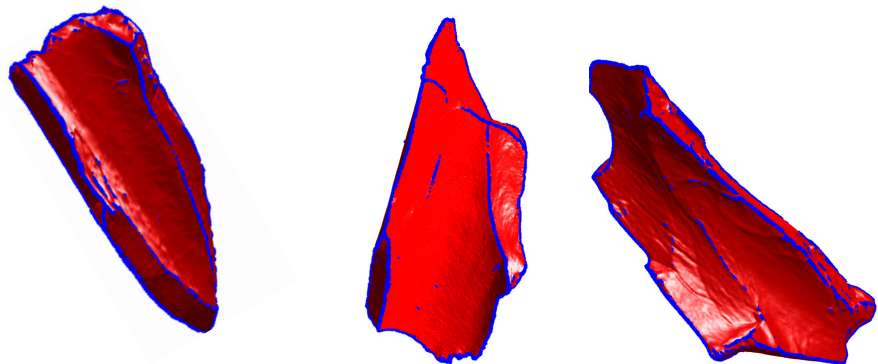


Figure: Results of edge detection via thresholding the spherical volume invariant 1 standard deviation below the mean.

Fracture edge detection

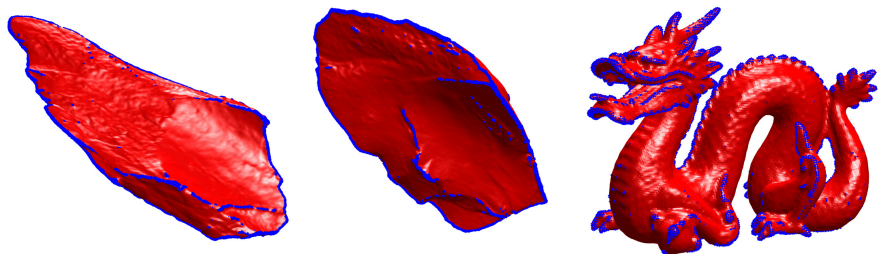


Figure: Results of edge detection via thresholding the spherical volume invariant 1 standard deviation below the mean.

Curent/Future Work

- 1 Use spherical volume invariant and machine learning to classify fragments by agent of breakage.
- 2 Automatic refitting of bone fragments.

Acknowledgements

- **Code:** <https://github.com/jwcalder/Spherical-Volume-Invariant>
- All simulations are the work of Riley O'Neill (University of St Thomas).
- Co-authors: Katrina Yezzi-Woodley (Anthropology, UMN), Professor Peter Olver (Mathematics, UMN), Pedro Angulo-Umana, Bo Hessburg, and Jacob Elafandi (Mathematics, UMN).
- The bone fragments depicted are from an adult elk (*Cervus canadensis*) femur that was broken by adult male spotted hyena (*Crocuta crocuta*) named Scruffy who resides at the Milwaukee County Zoo. The femur was disarticulated and defleshed prior to being fed to the hyena.
- All fragments were scanned with a DAVID white light scanner that was made available by the Evolutionary Anthropology Labs at the University of Minnesota.
- The authors also gratefully acknowledge discussions with Martha Tappen, Jacob Elafandi, and Jacob Theis.
- We gratefully acknowledge the support of the National Science Foundation under grant NSF-DMS grant 1816917.

Outline

1 Background

- Broken bones
- Differential and integral invariants

2 Spherical Volume Invariant

- Boundary integral formulation
- Computation
- PCA on local neighborhoods
- Experimental results

3 References



Calder, J. and Esedoğlu, S. (2012).
On the circular area signature for graphs.
SIAM Journal on Imaging Sciences, 5(4):1355–1379.



Manay, S., Hong, B.-W., Yezzi, A. J., and Soatto, S. (2004).
Integral invariant signatures.
In *European Conference on Computer Vision*, pages 87–99. Springer.



O'Neill, R., Angulo-Umana, P., Calder, J., Hessburg, B., Olver, P. J., Shakiban, C., and Yezzi-Woodley, K. (2019).
Computation of circular area and spherical volume invariants via boundary integrals.
arXiv preprint arXiv:1905.02176.



Pottmann, H., Wallner, J., Huang, Q.-X., and Yang, Y.-L. (2009).
Integral invariants for robust geometry processing.
Computer Aided Geometric Design, 26(1):37–60.



Pottmann, H., Wallner, J., Yang, Y.-L., Lai, Y.-K., and Hu, S.-M. (2007).
Principal curvatures from the integral invariant viewpoint.
Computer Aided Geometric Design, 24(8-9):428–442.



Yang, Y.-L., Lai, Y.-K., Hu, S.-M., Pottmann, H., et al. (2006).
Robust principal curvatures on multiple scales.
In *Symposium on Geometry Processing*, pages 223–226.